Ann. Geophys. Discuss.,
https://doi.org/10.5194/angeo-2020-45-AC1, 2020

Annales Geophysicae Discussions
Open Access

Interactive comment on "Fragmented Aurora-like Emissions (FAEs) as a new type of aurora-like phenomenon" *by* Joshua Dreyer et al.

Joshua Dreyer et al.

joshua.dreyer@irfu.se

Received and published: 21 October 2020

AR: We thank the referee for providing their helpful feedback! In the following, we respond (Authors' Response, blue) to each of the referee's comments (black) individually.

General Comments

The paper is well-written and organized. It presents interesting observations of short living small scale aurora-like structures of high scientific interest. The presented first summary for characteristic features of the discussed Fragmented Aurora-like Emissions is important for future follow-up studies. Instrumentation, observations and methods are well explained. The paper presents images and spectral data for FAEs strongly

Printer-friendly version

Discussion paper

supporting the author's hypothesis for a low energy generation mechanism with an upper energy limit between ∼8–11 eV which excludes a formation caused by precipitating electrons. The authors clearly state that the exact generation mechanism remains unclear. Their finding that FAEs are associated with elevated electron temperatures points to Farley-Buneman instabilities as a potential energy source and sets an important base for follow-up studies. I have only a few minor comments for the authors to consider a few minor additions prior publication.

AR: The above statement captures the aim of the present study very well and we are grateful that the referee acknowledges the scope of the paper as a "first report" to characterise the main characteristics of FAEs.

Specific comments

Major comments: No major comments.

Minor comments:

- It would be helpful to add a video showing an example for a category 2 FAE.

AR: We agree, but unfortunately we do not have an ASK video observation of category 2 FAEs at this time.

- L. 29–30: I recommend to add references for the following papers all presenting strong arguments against the hypothesis that precipitating electrons are responsible for picket fence structures below the purple arc of STEVE (Nishimura et al., 2019). Paper 1: Gillies D. M. et al. (2019). First Observations From the TREx Spectrograph: The Optical Spectrum of STEVE and the Picket Fence Phenomena, Geophysical Research Letters, 46 (13), 7207–7213. Paper 2: Mende S. B. & Turner C. (2019). Color Ratios of Subauroral (STEVE) Arcs, Journal of Geophysical Research: Space Physics, 124 (7), 5945–5955. Paper 3: Mende S. B., et al. (2019). Subauroral Green STEVE Arcs: Evidence for Low-Energy Excitation, Geophysical Research Letters, 46 (24), 14256–14262.

AR: We will add this argumentation and suggested references 2 and 3 against precipitation-caused picket fence structures to the revised manuscript for a more balanced discussion on this point. We would like to note that the suggested reference 1 (Gillies et al., 2019) does not conclude this and rather suggests that the picket fence structures are caused by particle precipitation, with typical auroral OI emissions dominating at 557.7 nm. This paper could thus be added as an additional reference for the viewpoint that the picket fence is likely an auroral feature.

- L. 47–48: The authors mention that similar structures (FAEs) have been sighted on Svalbard at other days. I recommend to mention on how many days FAEs have been identified.

AR: FAEs were observed at least on three other dates. Since we are not able to systematically search for these features in, for example, EISCAT data or optical images yet, identification of further events is currently based on manually reviewing auroral images. One of the main goals of the present study is to derive the main characteristics of FAEs to hopefully make the identification of further events easier, as the referee has correctly pointed out.

- L. 53–56: [...The images were taken using an exposure time of 4 s and an ISO of 16000 at a cadence of 11 to 12 s, with a mean interval length of 11.8 s. This variance is due to variations of the read-out time to the attached computer, with the camera exposure time set to 10 s...] Contradicting exposure times. What is correct, 4 s or 10 s? Please clarify.

AR: We apologize for this obvious error. The exposure time is 4 s, the longer cadence of $\sim$11.8 s is due to a readout delay between the camera and the third-party software on the connected computer. This will be corrected in the revised manuscript.

- Figure 4: This figure shows a mark for the zenith. Is this the local magnetic zenith? Please clarify.

AR: The marked zenith is not referring to the local magnetic zenith, but rather to the geographic zenith (centre of the ASC image). This was mainly used during the analysis to derive the pixel scale of the ASC images using an equisolid projection, as the fisheye lens will result in larger pixel-to-km-ratios further from zenith, which need to be accounted for. We will add a sentence to explain this in the revised manuscript.

- Figure 6 and 7: [...Data points with errors $>$ 50% of the values were removed...] What are the errors for the shown data points? Are they close to 50% or significantly less? Please clarify.

AR: The errors for the shown data points are mostly significantly less than 50%, further decrease of the filtering range (for example to $>$30%) does not remove significantly more data, none of which is at the time of the FAE passing. The errors for the period between 18:20–18:23 up to the FAE passing and above 100 km (which is the most relevant part for our analysis) are less than 20% of the values. We will add a similar concise statement to the revised manuscript.

Technical corrections: None

Interactive comment on Ann. Geophys. Discuss., https://doi.org/10.5194/angeo-2020-45, 2020.

Ann. Geophys. Discuss.,
https://doi.org/10.5194/angeo-2020-45-AC2, 2020

Annales Geophysicae Discussions

Open Access

EGU

Interactive comment on "Fragmented Aurora-like Emissions (FAEs) as a new type of aurora-like phenomenon" *by* Joshua Dreyer et al.

Joshua Dreyer et al.

joshua.dreyer@irfu.se

Received and published: 22 October 2020

AR: We thank the referee for providing their helpful feedback! In the following, we respond (Authors' Response, blue) to each of the referee's comments (black) individually.

In general, I disagree with the premise of the paper to create a name for an aurora-like phenomena, because the aurora in general contains so much natural variation and on a continuum of spatial and temporal scales. However, this does not invalidate the careful and thoughtful work that the authors have done in analyzing the available data for several specific auroral events. I do not want this paper rejected right out, but I would like to see less emphasis on trying to establish a new name for an aurora-like

Printer-friendly version

Discussion paper

phenomenon and more emphasis on the analysis of small-scale auroral features, which show interesting aspects when analyzed in such detail, for example multiple processes for electron acceleration happening in close proximity or even on the same field line at different places. It seems that the features discussed only happen in conjunction with aurora and are thus part of the aurora.

AR: We agree that the focus should not be on finding names for newly reported features, but since there is so much variation in the aurora it is much simpler to describe specific features when there is a named pointer associated with the particular discussed features.
However, aurora-related phenomena are not necessarily part of aurora. For instance, STEVE is not aurora, because studies have shown that it is not caused by particle precipitation. But it is sometimes accompanied by the green “picket fence“ structures, which many studies have suggested to be a particle precipitation feature, and thus aurora. As pointed out by referee 1, there are also examples of studies arguing that the picket fence is not precipitation-based. Locally generated features are certainly possible in a disturbed ionosphere, such as during the analysed events, and the available data suggest a different generation mechanism than particle precipitation.
A more thorough analysis of the electron acceleration processes would absolutely be of interest, but drawing clear conclusions about these processes at such small scales is very difficult with the available data. This is outside the scope of the present study, which aims to provide a general overview of FAE characteristics and hopefully point to a potential generation mechanism that further studies might then be able to analyse in more detail.

Specific comments:

Figure 1 does not show any clear evidence of anything other than a typical auroral display. Also, the actual features cannot be seen under the yellow areas overlaid on the image.

Printer-friendly version

Discussion paper

AR: This is true. Figure 1 shows "All 262 marked FAE candidates for event 3, overlaid on the first image of the series taken at 07:36:35 UT. [...]", as mentioned in the caption. The FAEs itself did not all occur at the time of this specific picture, which is simply the first in the analysed series for that date. Our aim with this figure is to show the distribution of these features over the all-sky camera (ASC) field-of-view and illustrate the variety of shapes and sizes. We will make this point more clear in the revised manuscript, in both the running text and caption of Figure 1.

Figure 3 also does not show anything convincing either. There is no scale to gauge the size of these features extracted from the all-sky camera images. How do these features differ from what has been termed enhanced aurora (see Hallinan, et al., 1985)?

AR: We agree that a pixel/length/degree scale on the side of one of the panels would be very helpful and will add this in the revised manuscript. While the enhanced aurora (EA; Hallinan et al., 1985) describes an enhanced emission in a thin height layer along (typically) a rayed auroral structure, FAEs do not have the vertical extent of the auroral rays associated with them. The observed FAEs were also clearly dislocated from the field lines of the adjacent "normal" auroral features. As EA shows a similar spectrum to normal aurora, FAEs lack the blue emission component, at least in the samples analysed in this study. Furthermore, EA has also been observed as a quasi-stable structure lasting for minutes, while none of the FAEs lasted for that long (generally less than a minute, often only a few seconds). Overall, this suggests that they are a different phenomenon. We will add a paragraph on the comparison to EA in the revised manuscript.

Section 2.1: Inadequate description of how these are identified (just identified by eye). This will generate selection biases and their identification in general is based on some thresholds visible in the images that depend on the sensitivity of the camera and the eye. For example, if a more sensitive camera were used, it is possible that a diffuse background of aurora would become visible and these spots are just localized enhancements of that background. How are they identified, what metrics are used to determine their boundaries, identifying them by eye is not good enough...and can easily introduce errors and biases.

AR: We agree that the methods/approach used for the identification should be described in more detail and will add this to Section 2.1 in the revised manuscript. In auroral physics visual identification is a standard approach, since there is no robust automatic auroral identification tool available. It does bring in some human-observer bias, which thus makes it important to document the selection criteria as accurately as possible. Visual thresholding is the first step to identify any auroral structures. It automatically means that we cannot claim that we have found all the features, but perhaps only the most intense ones. The manual identification process will introduce some errors, which we try to address by ordering the observations into confidence groups. As the characteristics of the higher and lower confidence groups agree well, we are confident that most candidates are observations of the same phenomenon, but concede that some other auroral features might have been falsely included in the lower confidence groups, as stated in the manuscript (line 181 ff.). The background aurora for FAEs, wherever existing, is red, and thus would not explain the observed green emission “blob” at lower altitudes.

Section 3.1: The paper mentions that the larger patches identified might just be diffuse auroral patches. Is it not possible that all of these FAEs might just belong to the general category of diffuse aurora? Pulsating / diffuse auroral patches have been found to have very limited altitude extent (see Stenbaek-Nielsen and Hallinan, 1979) and is believed to be a fairly common feature among the diffuse auroral structures.

AR: Pulsating patches do indeed have a limited altitude extent and they are very common (60% of the aurora at 3-5 MLT as estimated by Jones et al., 2011), but they occur within diffuse aurora. The analysed FAEs are seen alongside discrete arcs. Pulsating auroral patches are also typically much larger and very stable (e.g., Humberset et al., 2018; Nishimura et al., 2020) with the whole patch or a part of it undergoing quasi-periodic fluctuations in the emission intensity. However, FAEs are very short-lived (generally less than a minute, many just a few seconds) without any sign of obvious emission intensity fluctuations. The available ASK observations of FAEs also look markedly different from diffuse aurora and pulsating patches, as they are much smaller and show more dynamic motion. Overall, this suggests that they are a different phenomenon. We will add a paragraph on the comparison to pulsating/diffuse patches in the revised manuscript.

Line 152: Can you provide a reference that discusses the details of the electron energy estimate from that emission line ratio?

AR: This approach is explained in, for example, Lanchester et al. (2009), see the reference at line 158. We will add a reference also at line 152 in the revised version of the manuscript. It is commonly used with ASK data, other references are, e.g., Dahlgren et al. (2016), Whiter et al. (2010), Lanchester & Gustavsson (2013).

Line 180: I would not say that it is 'clear'. The data presented seem to just show normal variations within the diffuse aurora.

AR: We agree that the word "clear" should be avoided here and will rephrase this. The Discussion can be started by saying that "Fragmented Aurora-like Emissions have been studied [. . .]". We disagree that these features are just normal variations within diffuse aurora, as they show too many specific characteristics which do not fit well to any previously described phenomenon (see above response).

Line 184-185: It is not clear how the 'field-aligned emission extent' is measured. Parallax is not used, so is it just the off zenith viewing geometry of most of the all-sky FOV? If the latter is the case, there will likely be large uncertainty in the altitudes just based on the viewing geometry and what other auroral features could lie along the same line of sight at different altitudes. If it is the EISCAT signatures, then the wording should reflect the altitude of ionization and not auroral emissions.

AR: The lack of field-aligned extent is seen in the off-zenith parts of the optical ASC images, but the same is also suggested by the EISCAT electron density measurements of the FAEs at magnetic zenith. A precise determination of FAE altitudes is not possible with the available data, as we would either need observations from multiple locations or many more FAE signatures in EISCAT data, as discussed in line 186 ff. We will add "[...], as suggested by the off-zenith parts of the ASC images and field-aligned ionisation measured by the ESR, [...]" at line 185 in the revised manuscript.

Line 215-216: Is it not still possible that the O^+ density could be up to $\sim$10 times higher than the N_2^+ and O_2^+ densities in this altitude range?

AR: The O^+ density could be higher than the combined O_2^+, NO^+ and N_2^+ densities towards the upper end of this altitude range, and according to the International Reference Ionosphere (IRI) predictions for the date of event 3, O^+ is the dominant ion above $\sim$220 km. However, the point here is to give a lower limit of the electric field strength estimate. We cannot exclude that the IRI model underestimates the increase of molecular ions over O^+ towards higher altitudes that occurs at geomagnetically active times. In the most extreme case molecular ions could dominate even up to 300 km altitude. Even if we assumed m_i =16 (exclusively O^+ ions), it would only increase the estimated $E_\perp$ value by $\sim$37%. A more reasonable guess would be closer to m_i =22 (considering the very low O^+ abundances at the lower altitudes), which would result in a $\sim$17% increase of $E_\perp$. We will reformulate the statement to make it clearer that the estimated $E_\perp \approx$ 70 mV m^{-1} is a lower limit (if molecular ions are not dominating). In any case, a higher value would only further exceed the typical threshold for Farley-Buneman instabilities and thus not change the argumentation/conclusion for this point.

Lines 253-257: This paragraph summarizes the overall uncertainty and limitations of the data used in the current study, which limits the conclusions that can be drawn from them. Thus it is not scientifically sound to define a new feature with such a limited data set, especially without any clear metrics of how they are defined. Multitudes of auroral structures have been observed within both discrete and diffuse aurora for many

Printer-friendly version

Discussion paper

decades and only very few have been assigned specific names and those come mostly from historical reasons.

AR: It is important to be clear and honest about the limitations in the identification. However, hundreds of observations is not an insignificant number of features which do not fit into any earlier reported type of aurora. We will extend Section 2.1 to improve the metrics description and more clearly state how the events have been identified. As discussed above, visual identification of auroral features is a standard approach, and the aim of the present study is not to present a definite answer on the nature of FAEs or their origin, but rather to provide a first overview of their apparent characteristics based on the available data. Based on our analysis, we arrive at the conclusion that the observed features do not fit the characteristics of any previously reported auroral features, which is why we present them as a potential newly reported phenomenon. We disagree with the idea that features should not be named just because many other features do not have names yet. Naming and reporting on a rare and unexplained phenomenon is one of the first steps to gathering further observations and thus ultimately to understanding its formation mechanism.

References:

Hallinan, T. J., H. C. Stenbaek-Nielsen, and C. S. Deehr (1985), Enhanced aurora, J. Geophys. Res., 90, 8461–8475, doi:10.1029/JA090iA09p08461.

Stenbaek-Nielsen, H. C. and T. J. Hallinan (1979), Pulsating Auroras: Evidence for Non-collisional Thermalization of Precipitating Electrons, J. Geophys. Res., 84, 32573271.

Response references:

Jones, S. L., Lessard, M. R., Rychert, K., Spanswick, E., and Donovan, E. (2011), Large-scale aspects and temporal evolution of pulsating aurora, J. Geophys. Res., 116, A03214, doi:10.1029/2010JA015840.

Humberset, B. K., Gjerloev, J. W., Mann, I. R., Michell, R. G., & Samara, M. (2018). On the Persistent Shape and Coherence of Pulsating Auroral Patches. Journal of Geophysical Research: Space Physics, 123(5), 4272–4289. https://doi.org/10.1029/2017JA024405

Nishimura, Y., Lessard, M. R., Katoh, Y., Miyoshi, Y., Grono, E., Partamies, N., Sivadas, N., Hosokawa, K., Fukizawa, M., Samara, M., Michell, R. G., Kataoka, R., Sakanoi, T., Whiter, D. K., Oyama, S. ichiro, Ogawa, Y., & Kurita, S. (2020). Diffuse and Pulsating Aurora. Space Science Reviews, 216(1), 1–38. https://doi.org/10.1007/s11214-019-0629-3

Dahlgren, H., Lanchester, B. S., Ivchenko, N., & Whiter, D. K. (2016). Electrodynamics and energy characteristics of aurora at high resolution by optical methods. Journal of Geophysical Research: Space Physics, 121(6), 5966–5974. https://doi.org/10.1002/2016JA022446

Whiter, D. K., Lanchester, B. S., Gustavsson, B., Ivchenko, N., & Dahlgren, H. (2010). Using multispectral optical observations to identify the acceleration mechanism responsible for flickering aurora. Journal of Geophysical Research: Space Physics, 115(12), 1–10. https://doi.org/10.1029/2010JA015805

Lanchester, B. and Gustavsson, B. (2013). Imaging of Aurora to Estimate the Energy and Flux of Electron Precipitation. In Auroral Phenomenology and Magnetospheric Processes: Earth And Other Planets (eds A. Keiling, E. Donovan, F. Bagenal and T. Karlsson). doi:10.1029/2011GM001161

Interactive comment on Ann. Geophys. Discuss., https://doi.org/10.5194/angeo-2020-45, 2020.

Printer-friendly version

Discussion paper

Relevant changes:
Implementation of referees' comments, mainly:
1. Expansion of Section 2.1 (Methods)
2. Expansion of Section 4 (Discussion) to include comparison to other auroral phenomena
Various minor changes were included. Additions to the prior version are marked in blue, deletions in red.

Characteristics of Fragmented Aurora-like Emissions (FAEs) ~~as a new type of aurora-like phenomenon~~observed on Svalbard

Joshua Dreyer[1,2], Noora Partamies[3,4], Daniel Whiter[5], Pål G. Ellingsen[6], Lisa Baddeley[3,4], and Stephan S. Buchert[1]

[1]IRF Swedish Institute for Space Physics, Space Plasma Physics group, Uppsala, Sweden
[2]Uppsala University, Department of Physics and Astronomy, Uppsala, Sweden
[3]The University Centre in Svalbard, Longyearbyen, Norway
[4]Birkeland Centre for Space Science, Bergen, Norway
[5]University of Southampton, Southampton, UK
[6]UiT The Arctic University of Norway, Department of Electrical Engineering, Narvik, Norway

Correspondence: Joshua Dreyer (joshua.dreyer@irfu.se)

Abstract. This study analyses the observations of a new type of small-scale aurora-like feature, which is further referred to as Fragmented Aurora-like Emission(s) (FAEs). An all-sky camera captured these FAEs on three separate occasions in 2015 and 2017 at the Kjell-Henriksen Observatory near the arctic town of Longyearbyen, Svalbard. A total of 305 FAE candidates were identified~~with varying degrees of certainty.~~. They seem to appear in two categories - randomly occurring individual FAEs and wave-like structures with regular spacing between FAEs alongside auroral arcs. FAEs show horizontal sizes typically below 20 km, a lack of field-aligned emission extent and short lifetimes of less than a minute. Emissions were observed at the 557.7 nm line of atomic oxygen and at 673.0 nm (N_2, first positive band system), but not at the 427.8 nm emission of N_2^+ or the 777.4 nm line of atomic oxygen. This suggests ~~a~~ an upper limit to the energy ~~of~~ that can be produced by the generating mechanism. Their lack of field-aligned extent indicates a different generation mechanism than for aurora, which is caused by particle precipitation. Instead, these FAEs could be the result of excitation by thermal ionospheric electrons. FAE observations are seemingly accompanied by elevated electron temperatures between 110–120 km and increased ion temperatures at F-region altitudes. One possible explanation for this are Farley-Buneman instabilities of strong local currents. ~~We~~ In the present study we provide an overview of the observations and discuss ~~them~~ their characteristics as well as potential generation mechanisms~~in the present study.~~.

1 Introduction

Aurora as a phenomenon has been studied extensively over the past century, and mesoscale auroral forms like arcs are generally rather well-understood. Some open questions remain though, such as the intricacies of sudden changes in morphology and the drivers behind dynamic auroral processes (Karlsson et al., 2020). Small-scale features on the other hand are much less well-known and new features are still being found, for example transient phenomena such as Lumikots (McKay et al., 2019).

Auroral emission is dependent on the atmospheric composition, which varies with altitude. The same wavelengths that are typically observed with aurora can also be emitted without the presence of particle precipitation. One such example is airglow, which can produce the same 557.7 nm and 630.0 nm emission lines of atomic oxygen as typical aurora, but in this case due to dissociative electron recombination (e.g. Peverall et al., 2000). Interaction between aurora and the dynamics of the neutral atmosphere is a complex subject, with features such as the recently discovered *dunes* potentially being caused by atmospheric wave modulation on diffuse aurora (Palmroth et al., 2019). Thus, not all emissions similar to aurora are caused by particle precipitation, with Strong Thermal Emission Velocity Enhancement (STEVE) being already a well-known example of aurora-like skyglow, which is likely caused by local acceleration processes instead of precipitation (Gallardo-Lacourt et al., 2018). It is sometimes accompanied by green rays known as picket fence below the purple arc of STEVE (MacDonald et al., 2018). ~~Nishimura et al. (2019) have shown this picket fence to be likely~~ This picket fence is ostensibly related to particle precipitation ~~, whereas STEVE itself is~~ (Nishimura et al., 2019; Gillies et al., 2019), although some studies have questioned this connection based on spectral analysis (Mende and Turner, 2019; Mende et al., 2019). STEVE itself has been associated with subauroral ion drifts and local electron heating (MacDonald et al., 2018).

In this study we suggest Fragmented Aurora-like Emissions (FAEs) as another phenomenon in the same category of aurora-like phenomena, for which particle precipitation is unlikely to be the direct cause. The small fragments of excited plasma discussed in the present study seem to differ from other auroral structures in various ways. They exhibit small horizontal scales of only a few kilometres, short lifetimes of generally less than a minute and a lack of field-aligned emission extent. Generally, the FAEs occur close to auroral features. This is especially true for FAEs of the second type, occurring in wave-like structures, which were observed with an offset to auroral arcs on the same scale as the FAE size. The next section of the present study aims to provide an overview of the observations and instrumentation used to gather data, followed by a more in-depth description of FAE characteristics. Finally we suggest some potential generation mechanisms and relations to other recently discovered aurora-like phenomena and summarise our conclusions.

2 Instrumentation and observations

All of the analysed FAEs were observed on all-sky camera (ASC) images captured at the Kjell Henriksen Observatory (KHO), which is located on the Breinosa mountain east of Longyearbyen, Svalbard at ∼78.15° N, 16.04° E. The first observation was made on 2015-11-07 between 20:15:58 UT and 20:17:27 UT, with 4 identified FAE candidates over 4 images (further referred to as "event 1"). ~~They~~ FAEs were next seen again on 2015-12-07 between 18:18:14 UT and 18:27:36 UT (20 images, "event 2"), this time a total of 39 candidates. The final observation that is analysed in the present study was made over a much longer period on 2017-12-18 between 07:36:35 UT and 08:26:48 UT, consisting of 79 images ("event 3") in which 262 candidates were marked. Figure 1 shows all these marked candidates for event 3 overlaid on the first image of the series taken at 07:36:35 UT. This is done to visualise the distribution across the sky and general characteristics of the marked candidates, almost all occurred at a later time during event 3. All FAE events were accompanied by aurora. It should be noted that ~~these~~ FAEs have also been sighted ~~on Svalbard at~~ at the KHO on at least three other dates, which were more recent and thus not included in the present study.

Due to the availability of varied instrumentation on Svalbard, an effort was made to incorporate many different data sources to obtain FAE characteristics. These include the Sony α7S all-sky camera (ASC) and meridian-scanning photometer (MSP) at the KHO, as well as data from the European Incoherent Scatter Scientific Association (EISCAT) Svalbard Radar (ESR) (Wannberg et al., 1997) and high-framerate optical observations with the Auroral Structure and Kinetics (ASK) instrument (Dahlgren et al., 2008) located at the ESR. The ASC images used in the present study have a size of 2832 $\times$ 2832 pixels. The images were taken using an exposure time of 4 s and an ISO of 16000 at a cadence of 11 to 12 s, with a mean interval length of 11.8 s. This variance is due to variations of the read-out time to the attached computer~~, with~~. The readout delay between the camera and software is responsible for the slower cadence, compared to the camera exposure time~~set to 10 s~~. A simple astrometry calibration was used to find the centre of the ASC images and estimate the pixel size, resulting in a scale of 16.59 pixel/degree close to centre. This is further used to determine the offset of FAEs from zenith, which can then be used to calculate the pixel sizes in km for varying elevation angles, using an equidistant projection ~~, at~~ and an assumed FAE altitude of 110 km. This assumption was based on FAE signatures in the ESR data.

Spectral information is provided by the MSP, which is scanning the auroral emissions ~~in Rayleigh~~ at 427.8 nm (N_2^+), 557.7 nm and 630.0 nm (both atomic oxygen) with a 1°field of view (FOV) from north to south along the local geomagnetic meridian (31° west of geodetic north) using a rotating mirror. Measurements have a time resolution of 8 s (16 s for events 1 and 2), consisting of 4 s (8 s) for a full 360° scan plus another 4 s (8 s) for a background scan. Thus, scanning across the sky takes 2 s (4 s). The background measurement is achieved by tilting a narrow band-pass ($\sim$0.5 nm) interference filter for each channel (Chen et al., 2015).

High temporal resolution optical observations from ASK are used to further study the movement and emission properties of the FAEs. ASK consists of three channels with individual band-pass filters for selected auroral wavelengths and lenses to adjust FOV (Ashrafi, 2007). This allows for simultaneous observations of different auroral emissions in a narrow FOV, which can be used to study the energy and flux of the precipitating electrons that produce the aurora (Lanchester et al., 2009). The temporal resolution is 20–32 Hz, and for resolutions above 5 Hz, the available 512 pixels for each camera are binned into a 256 $\times$ 256 pixel image (Goodbody, 2014). ASK is pointing towards the magnetic zenith and shares part of its observation region with the ESR and the MSP, which led to a finding of a FAE signature in the ESR data after observing ~~a passing in~~ its passing across the FOV of ASK. The ASK FOV is 6.2° and in this study we use observations of N_2 (673.0 nm, first positive band system) and atomic oxygen (777.4 nm) emissions.

Solar wind data from the Advanced Composition Explorer (ACE) and Deep Space Climate Observatory (DSCOVR) satellites at the L1 Lagrangian point can provide insight into the background conditions during the observed events. For the periods preceding the two larger events (2 and 3) the ACE and DSCOVR data show average speeds of ~~620-640~~620–640 km/s, which is above the ~~usual~~ threshold value for high-speed streams (Cranmer, 2002). The B_z component of the Interplanetary Magnetic Field (IMF) is negative and IMF B_y is positive for the relevant periods preceding the FAE occurrences. This indicates an efficient energy transfer into the magnetosphere-ionosphere system. The ACE data for event 1 show average solar wind speeds of ~ 540 km/s, negative IMF B_z, both of which resemble the other two events to some degree, but negative IMF B_y. The K_p indices for the time periods of events 1–3 are 3+, 4- and 4+, indicating moderate geomagnetic activity. Visually inspected convection maps from SuperDARN radars suggest an ionospheric plasma flow primarily in the northwest or southwest direction. For all our event times Svalbard was located in the evening cell of the convection and close to the flow reversal.

2.1 Methods

The FAE candidates appearing on the ASC images were visually identified and ~~marked by eye, with the~~ manually marked, using the freehand selection tool of the Fiji distribution of the freely available ImageJ software (Rueden et al., 2017; Schindelin et al., 2012)~~, using the freehand selection tool . This~~. After inspecting the entire image set, the criteria to mark the candidates were identified as outline clarity and strength of the emission intensity enhancement, size, apparent vertical extent and movement across successive pictures. Generally, FAE candidates are clearly offset from the adjacent aurora as emission intensity enhancements confined in a small region, with little to no apparent vertical extent visible in the ASC images. Their limited lifetime results in each individual candidate typically only being visible in 1–4 successive images, with longer lasting candidates showing discernible movement between images. Their short-lived nature often makes identification of newly appearing FAEs relatively obvious when comparing two successive images. Due to the mean cadence of 11.8 s, it is not easy to track FAEs between each image. The term "candidate" in this context refers to a suspected FAE on each individual image, with some of the more stable candidates almost certainly being the same FAE on successive images. While visual identification will certainly introduce some human-observer bias, it is nonetheless a standard approach in auroral studies, since there is no robust automatic identification tool available. It is possible that only the most intense features were identified, but given the large amount of FAE candidates, they should be sufficient to derive the main characteristics of FAEs.

This identification process resulted in a compiled database with all candidates containing their outlines, pixel coordinates and sizes. A total of 305 candidates were marked for further analysis and categorised into 4 confidence groups, depending on their intensity, size and outline characteristics. Group 1 is composed of the most well-defined candidates with clear borders and strong intensity enhancements, whereas candidates in groups 2-4 are of decreasingly lower quality, meaning they are more likely to contain features that are for example part of an auroral arc. The 21 FAEs of the highest quality form group 1, whereas group 2 contains 55 candidates. These 76 candidates are considered as the core set of observations. Group 3 contains 78 candidates and group 4 encompasses 151 candidates. FAEs in groups 3 and 4 are analysed in the same manner, but only contribute to the final conclusions if they agree with the core set findings, which would indicate that these are indeed observations of the same phenomenon.

3 FAE characteristics

FAEs can be categorised into two distinct categories, the first being individually occurring FAEs. These occur seemingly randomly across the sky, sometimes with a significant offset to the closest auroral arc. The second type are periodic structures with regular spacing between FAEs, which appear close to and generally northwards of auroral arcs. The category 2 FAE group shown in Figure 3 is a typical example.

3.1 Distribution, sizes and movement

For the three observed events, most FAEs (73.1%) occurred west of zenith. This is the case for both high- and low-quality candidates, with the dashed kernel density estimation (KDE) in Figure 1 for FAEs of groups 1 and 2 agreeing with the overall distribution KDE. Due to the observational bias caused by the vast majority (262) of FAEs occurring during event 3, this asymmetry in FAE location on the sky might simply be explained by the underlying space weather and ionospheric convection conditions being biased towards westward convection during this period. The low number of FAEs close to zenith (see Figure 1) is possibly explained by observational bias, since FAEs near zenith are harder to identify. Their lack of field-aligned emission extent is not visible when viewed from directly underneath. In addition, most FAEs occurred close to auroral arcs, which rarely appeared close to zenith during the analysed events. The location of category 1 FAEs appears to be fairly random and not necessarily close to auroral arcs, whereas category 2 FAE groups generally appear within the vicinity northwards of an arc, typically with an offset on the scale of the fragment size, corresponding to a few kilometres. Visual inspection of all events shows that FAEs appear mostly elliptical, thus fitting an ellipse to follow the marked outline of each FAE provides a more robust estimate of its size. As shown in Figure 2, the fitted ellipses of most FAEs have a major axis of 20 km or less, with a few larger outliers that might simply be diffuse auroral patches, especially on the larger end of the marked size range. The average major axis length is ~6–8 km, with an average minor axis of ~3–4 km. Their aspect ratio (AR $=$ [Major axis]$/$[Minor axis]) has a mean value of 2.04. Most FAEs seem to have fairly regular, rounded shapes with few indents, with a mean circularity value of $c = 0.705$ ($c = 1$ being perfectly circular), which is determined using the formula $c = 4\pi \cdot [\text{Area}]/[\text{Perimeter}]^2$. This determination is of course affected by their size, with deviations from rounded shapes being harder to identify in smaller FAEs, with an added general operator bias to outline regular shapes compared to complex indents. It should be noted that due to the 4 s integration time of the ASC, any fast-moving object will appear somewhat elliptical. Nevertheless, this is not true for the high-framerate data from ASK, which also show FAEs to be elliptical. The described trends are observable in both high- and low-quality candidates, as KDEs for high-quality FAEs are in good agreement with the entire data set in Figure 2. This suggests that most of the marked candidates of groups 3 and 4 are indeed FAEs. Category 2 FAEs can be seen moving along the auroral arc in Figure 3. The distance between these FAEs does not vary significantly as they move eastward over a period of 35 seconds. A spatial intensity variation is visible in the grouped structure, where FAEs appear dim towards the edges of the group and become more intense the closer they move towards the centre. Some of the variation in intensity seems to be caused by fragments appearing and disappearing at the ends of the group. Using an average distance of 45 pixels between the FAEs and their approximate elevation angle of $\sim 65^\circ$, we can roughly estimate the spacing between FAEs for this group to be

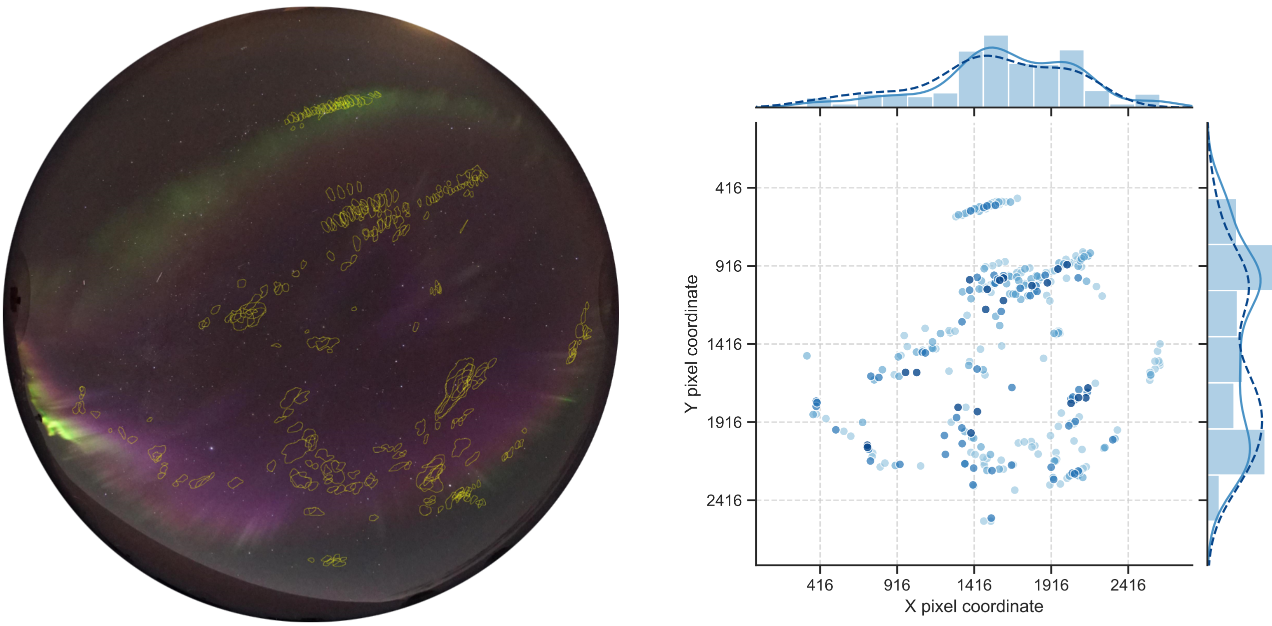

Figure 1. Left: All 262 ~~marked~~ identified FAE candidates for event 3 on 2017-12-18, overlaid on the first image of the series taken at 07:36:35 UT. The FAE candidates occurred over a time period of ∼50 minutes. Geomagnetic east corresponds to the left side of the image, geomagnetic north to the top. Right: All 305 FAE locations in horizontal and vertical pixel coordinates with histogram distribution and kernel density estimation (KDE). FAEs are shaded according to confidence groups, with darker shades being FAEs of higher quality. The dashed KDE line is only calculated for FAEs of groups 1 and 2. Credit: ASC image provided by the KHO.

around ∼ 6 km. Visual inspection of the ASC images shows a general westward movement of the FAEs for the observed events, which might originate from the underlying convection pattern. No obvious eastward motion was observed. A few FAEs were observed in the ASK high-framerate images (see Figure 5), with some remaining stable for multiple seconds while they drift, whereas others appeared and vanished within a second. The ASK FOV corresponds to 10×10 km^2 at an altitude of 100 km, which FAEs passed within ∼10–14 s. This results in an estimated drift speed on the order of ∼1 km/s.

3.2 Observed emissions

For FAE positioned along the MSP scanning line, the MSP data were checked to search for corresponding signatures. ~~At least three~~ Three FAE signatures were found, of which one is presented in Figure 4. Distinct FAE emissions were observed at the 557.7 nm (green MSP channel) line of atomic oxygen, but not at the 630.0 nm (red channel) line of atomic oxygen, nor at the 427.8 nm (blue channel) emission of N_2^+. Due to the long lifetime of the 630.0 nm emission state (∼110 s) and the short-lived and fast-moving nature of FAEs, the respective MSP red channel measurements are unlikely to show any distinct FAE signatures, with any potential emissions "smeared" over the temporal axis. Figure 4 shows a clear peak at the FAE elevation of ∼100° in the 557.7 nm measurements while it passed the MSP scan line (marked by vertical lines), with a clear drop-off as the

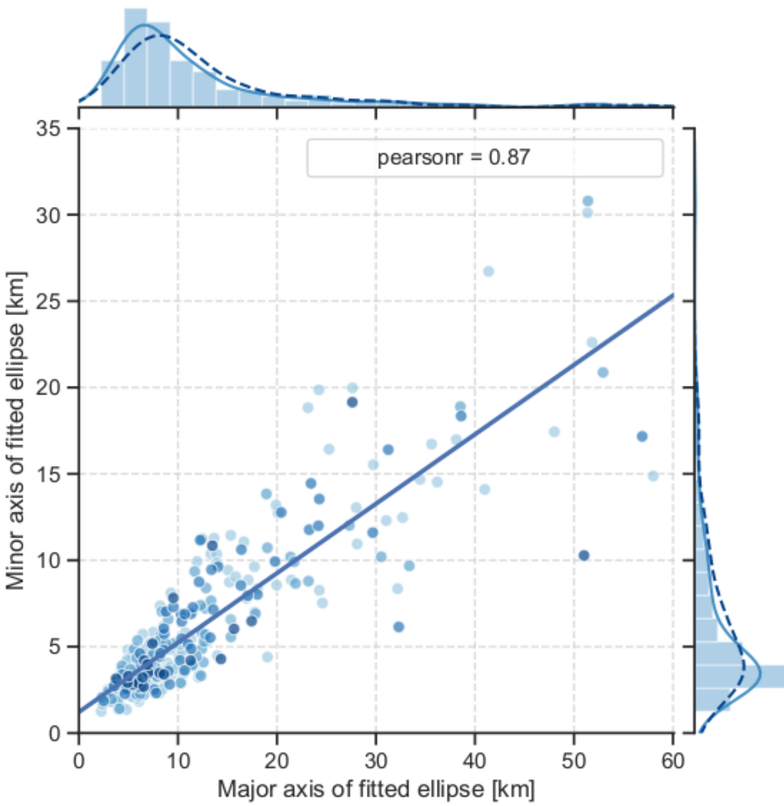

Figure 2. Length of major and minor axes (in km) of fitted ellipses for each FAE, assuming an altitude of 110 km. FAEs are shaded according to confidence groups, with darker shades being FAEs of higher quality. A histogram of the variables is plotted on the outer axes, together with a KDE. The dashed KDE line is only calculated for FAEs of groups 1 and 2. The legend shows the calculated statistical Pearson correlation coefficient for a linear regression, with a p-value $\ll 0.01$, rejecting the null hypothesis.

FAE moved out of the scan and faded. No distinct signature can be seen at this elevation in the 427.8 nm measurements~~(which are weaker in general) and only a~~. A broad general increase is visible over a large area in the 630.0 nm emissions, likely by the background aurora at higher altitudes, as this emission was elevated before and after the FAE occurrence. Also, at the suggested FAE altitude of $\sim$110 km, the atomic oxygen state which emits at 630.0 nm is heavily collisionally quenched and thus any FAE emissions at this wavelength at low altitudes are expected to be extremely weak. It should nonetheless be noted that the broad increase may potentially hide a FAE signature in the 630.0 nm data. The other MSP passings show comparable results.

~~At least one FAE was~~ One FAE was observed passing through the ASK FOV during event 2 on 2015-12-07 ~~(for the corresponding video file see Whiter (2020)), which provides much higher~~ (for the corresponding video file see Whiter, 2020). The ASK instrument provides temporal and spatial ~~resolution observations. It shows~~ high-resolution observations. N_2 emission

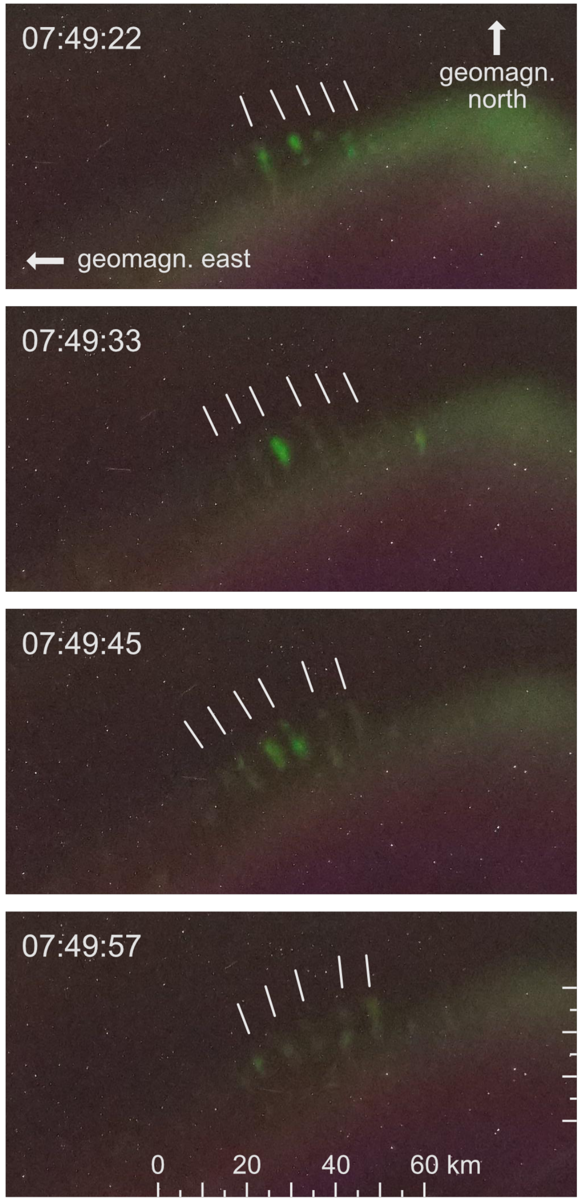

Figure 3. Movement of a category 2 FAE group northwards of the main auroral arc (northwest of zenith) over four successive images taken on 2017-12-18 around 07:49:40 UT. The images are cropped to ~~1250~~ 1000 × ~~660~~ 500 pixels to make the FAEs easily identifiable. White lines indicate the apparent alignment of the FAEs and were used to determine approximate distances between them. A scale in kilometre is added for reference, using a pixel to km ratio of 0.129 (at 65° elevation angle). Credit: ASC images provided by the KHO.

signatures at 673.0 nm (first positive band system) in the ASK channel 1 data ~~, as~~ can be seen in the left and middle panel in the bottom row of Figure 5. At the same time, no emission is visible in the right panel in the bottom row, which shows the

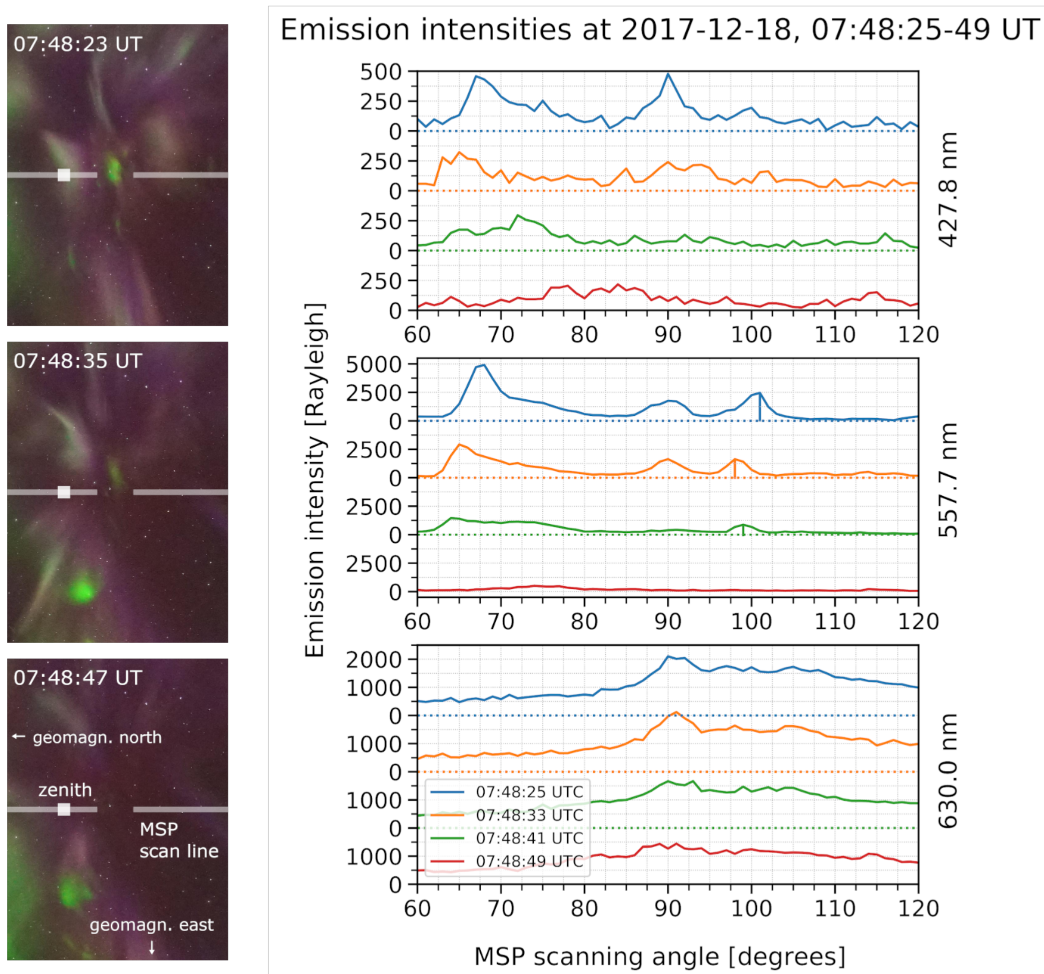

Figure 4. Comparison of consecutive cropped ASC images and MSP line scans for a FAE moving through the MSP scan line on 2017-12-18 between 07:48:23–47 UT. The FAE signatures are marked with vertical lines in the green channel (557.7 nm). The MSP scan line (1° width) is drawn on the ASC images in grey. A grey square marks the geographic zenith in the centre of the ASC images. Credit: ASC images provided by the KHO.

ASK 3 channel measuring at 777.4 nm (atomic oxygen). The ratio between 777.4/673.0 nm emissions is commonly used to determine the energy of precipitiating particles, and typically the lack of 777.4 nm emissions ~~and thus resulting very small ratio~~ resulting in very small ratios would mean high energy precipitation (e.g., Lanchester et al., 2009; Dahlgren et al., 2016). But even with very high energies, there should be some 777.4 nm as well as 427.8 nm emissions. The apparent lack of these emissions suggests a different generation mechanism than precipitation. As the FAEs show emissions at 557.7 nm and 673.0 nm, but seemingly not at 427.8 nm or 777.4 nm, looking at the excitation thresholds of these emissions can give a clue towards the upper energy limits of the generation mechanism. Excitation thresholds for the 427.8 nm and 777.4 nm emissions lie above 10 eV (e.g., Lanchester et al., 2009; Holma et al., 2006), with the lowest possible excitation energy being ∼11 eV for ~~777.4 nm emissions from~~ direct excitation of atomic oxygen at 777.4 nm. For the observed 557.7 nm and 673.0 nm emissions ~~they~~ the excitation energies are 2 and ∼8 eV, respectively (e.g., Holma et al., 2006; Ashrafi et al., 2009). Combined, this suggests an upper limit for the energy of the generation mechanism between ∼8–11 eV.

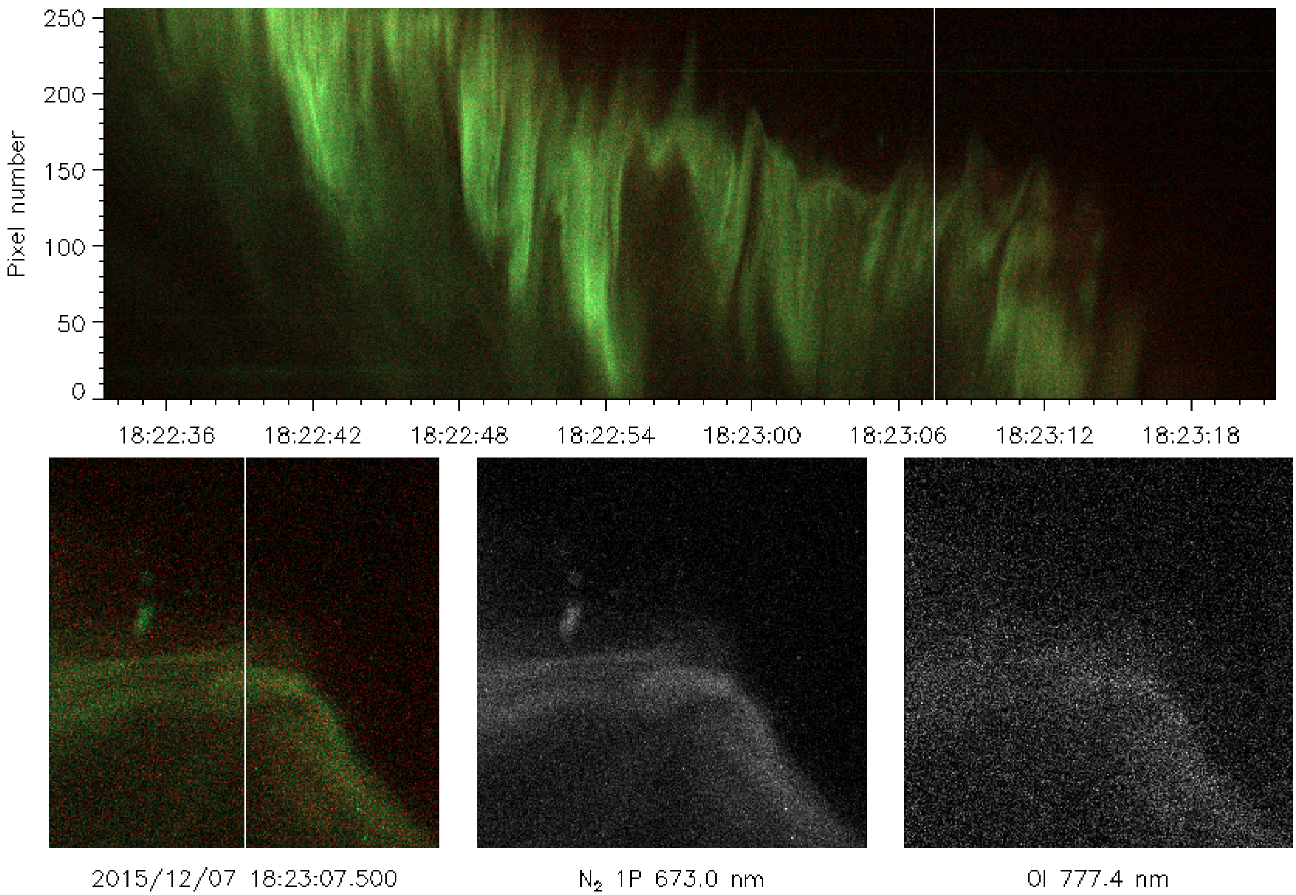

Figure 5. ASK keogram for the event of 2015-12-07 around 18:23:07 UT in the upper panel. ASK1 measuring the 673.0 nm emission of the first positive band system of N_2 is visible in the lower middle panel, the lower right panel shows the ASK3 measurement of 777.4 nm emissions of atomic oxygen, and the lower left panel shows ASK1 in the green/blue channel and ASK3 in the red channel.

3.3 Plasma characteristics measured with the ESR

To further understand the underlying plasma properties of FAEs, an attempt was made to find signatures within incoherent scatter data of the ESR. The auroral arc visible south of the FAE in Figure 5 extended across the entire FOV of ASK (partially shared with the ESR) shortly before the FAE occurrence at 18:23 UT, and is visible in Figure 6 as a general increase in electron density across the entire altitude range. The density decreases across most altitudes as the arc moves out of the FOV towards

18:23 UT. It remains high at 113 km at the time of the FAE occurrence. No associated increase in electron temperatures is visible in Figure 6 for the period and altitudes of the arc signature in the electron density panel.

The FAE visible in Figure 6 shows as a local increase in electron temperature to ∼2300 K at 113 km around 18:23 UT. This increase seems to be confined to a narrow altitude range, which is further established by the time series at four successive altitudes shown in Figure 7. The increase at the time of the FAE passing is limited to altitudes below 119 km and strongest at 113 km. For the period directly after the FAE occurrence, multiple increases in electron temperature are visible at low altitudes, which indicates an unstable lower ionosphere. Simultaneous increases in ion temperatures are visible at higher altitudes, with significant increases around 190 km, up to ∼4500 K.

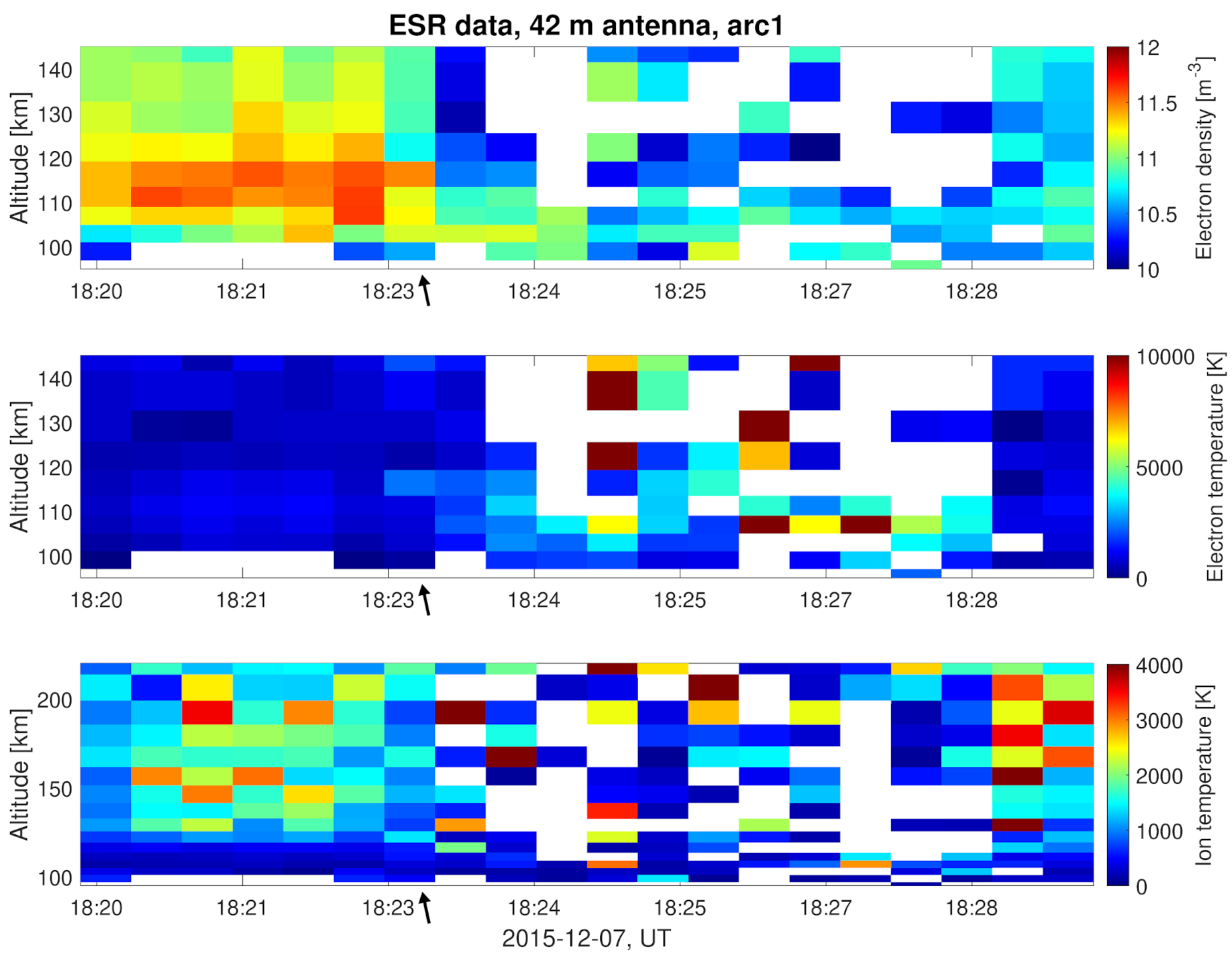

Figure 6. Incoherent scatter data from the ESR (analysed with GUISDAP) for 18:20–18:30 UT on 2015-12-07, with electron densities in the upper, electron temperatures in the centre and ion temperatures in the lower panel. Data points with errors $> 50\%$ of the values were removed. Further limiting to $> 30\%$ would only remove a few extra data points. Errors for the relevant time periods up to the FAE passing are $< 20\%$ of the values. The arrows mark the time of the FAE passing.

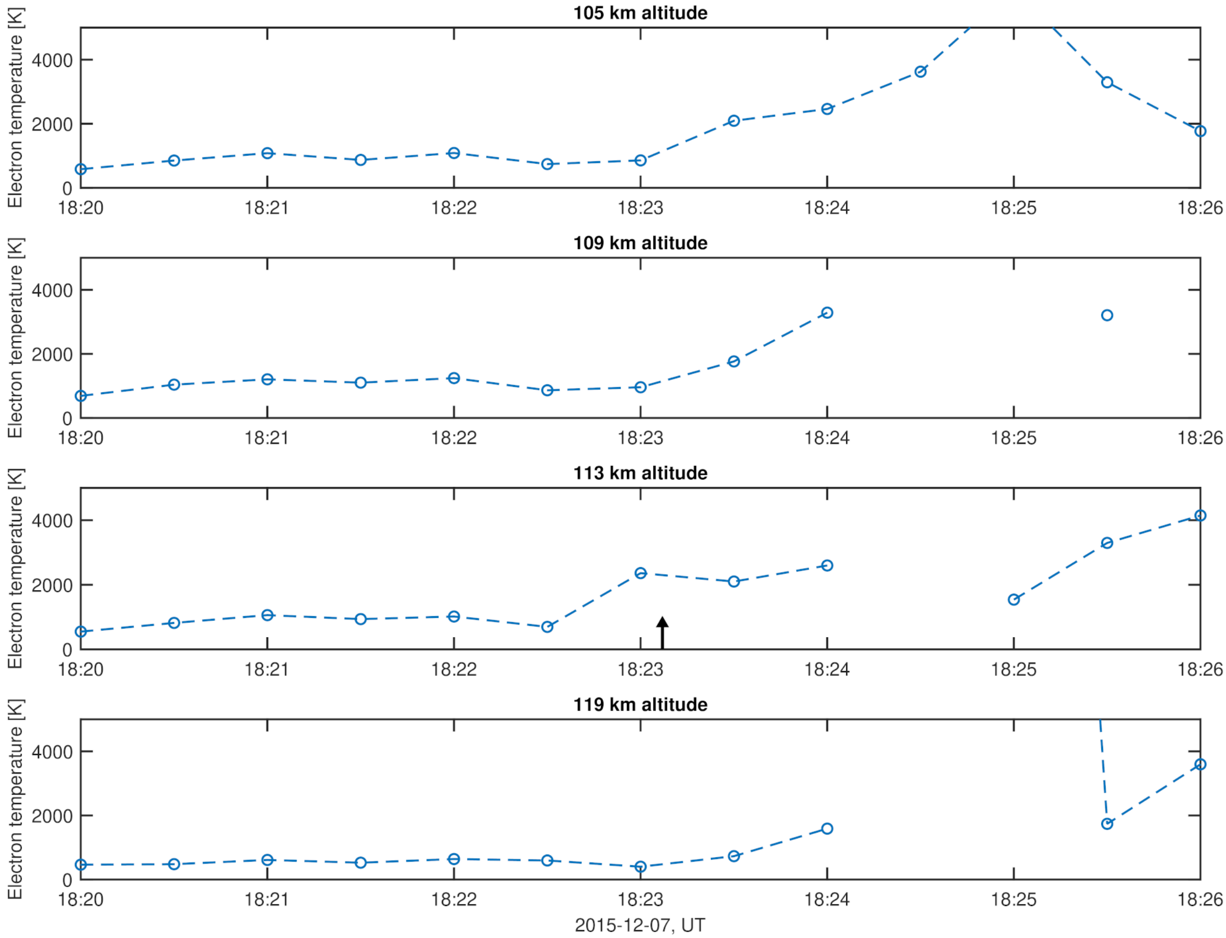

Figure 7. Time series of electron temperatures at four successive altitudes between 105–119 km from incoherent scatter data from the ESR (analysed with GUISDAP) for 18:20–18:26 UT on 2015-12-07. Data points with errors > 50 % of the values were removed. The arrow marks the time of the FAE passing and denotes the distinct increase in electron temperature specifically at 113 km.

The background conditions during these analysed events might be able to further provide some insight into the underlying generation mechanism. For the entire duration of event 3, significant intermittent increases in electron temperatures were observed at altitudes in the E-region, as well as elevated ion temperatures (mostly) in the F-region. This ~~seems to indicate~~ indicates a connection between FAEs and elevated electron temperatures at low altitudes, which we will discuss below.

4 Discussion

~~From the presented measurements it is clear that a new~~ Fragmented aurora-like ~~phenomenon~~ emissions have been analysed and classified in the present study, with results suggesting that they are a new type of aurora-like feature. Comparing FAEs with ostensibly similar auroral phenomena shows some key differences. For example, the term enhanced aurora (EA; see Hallinan et al., 1985) describes an enhanced emission in a thin layer, typically along a rayed auroral structure. Albeit also designating a localized emission intensity enhancement occurring alongside aurora, EA differs in various characteristics. EA occurs as layers with limited vertical extent, but longitudinal and latitudinal extents of at least 250 km and 300 km, respectively (Hallinan et al., 1985) . FAEs are much smaller, with minor and major axes sizes of < 10 km. While EA manifests as intensity enhancements along the rays of a bigger auroral feature, FAEs were clearly dislocated from the field lines of the adjacent rayed structures. FAEs also lack the blue emission enhancement visible in EA. Furthermore, EA has been observed ~~.~~ as quasi-stable structures lasting for minutes, while most analysed FAEs had lifetimes of less than a minute. Overall, this suggests that these are two different phenomena.

When comparing FAEs with pulsating patches, two major distinctions between the two phenomena are size and lifetime of the individual features. Pulsating patches occur within diffuse aurora, whereas the analysed FAEs are seen alongside discrete arcs. FAEs are much smaller than pulsating patches, which are also typically very stable, while showing quasi-periodic fluctuations in their emission intensity (e.g., Humberset et al., 2018; Nishimura et al., 2020). In contrast, FAEs are short-lived and do not show any emission intensity fluctuations, apart from appearing and fading away. The available ASK video observations of FAEs show their much higher dynamic motion and smaller size, compared to pulsating patches. Together, these differences lead us to conclude that FAEs are a distinctly different phenomenon.

As the FAEs were found by manual inspection of images, there is some bias in which features were selected and how they were classified. The data set could contain other auroral small-scale forms or diffuse patches, which is the reason for the classification into four confidence groups. As the general properties of candidates between high- and low-confidence groups agree well, we are confident that most selected features are indeed FAEs. Generally, FAEs can be distinguished from other auroral forms by their lack of field-aligned emission extent, as suggested by the off-zenith parts of the ASC images and field-aligned ionisation measured by the ESR, small sizes and short lifetimes. A FAE signature is visible in the ESR data as locally enhanced electron temperatures around 113 km. Determining a definite FAE altitude requires triangulation, which was not possible for the analysed ASC images, or other means of consistently identifying FAE signatures in measurements over an altitude range, such as multiple signatures in EISCAT data. ~~The present~~

Semeter et al. (2020) recently described green "streaks" below STEVE, which show various similarities to FAEs. Their triangulation positions the streaks at an altitude of 100–110 km, which is also the region we suggest FAEs to occur within. They propose superthermal electrons resulting from the extreme electric fields during STEVE as a local generation mechanism, similar to our hypothesis. It will be interesting to see if these two phenomena are indeed related on a fundamental level, or just bear superficial resemblance. Gallardo-Lacourt et al. (2018) suggest STEVE as another locally generated skyglow without any associated particle precipitation. The phenomenon is far from well-understood and occurs on much larger scales than FAEs, but indicates that ionospheric processes can indeed cause emission without particle precipitation being present. We propose that FAEs fall within the same category, even though many of their properties such as size and lifetime differ majorly. The underlying processes heating the plasma are unlikely to be the same, but on a fundamental level both emissions seem to be related to thermal ionospheric processes rather than particle precipitation.

The present study aims to present the basic characteristics of FAEs and categorise them based on the three analysed events. Nonetheless, the available data enable us to hypothesise about their underlying generation mechanism. The analysed events show above-average solar wind speeds (except for event 1), negative IMF B_z and positive B_y, with a westward convection of FAEs. They are not limited to a certain time sector, with occurrences both between 10:30-11:30 MLT and 21:15–23:15 MLT. The elevated electron temperature at E-region altitudes and simultaneous increases in ion temperatures at higher altitudes can provide some clues towards the origin of FAEs.

One possible group of generation mechanisms for the required energy to excite FAEs are Farley-Buneman instabilities, which are streaming instabilities typically occurring at altitudes of 90–120 km (Oppenheim et al., 1996). The proposed FAE altitude falls within this region. They become significant when the difference between electron and ion drift speeds exceeds the ion acoustic speed (Liu et al., 2016), which is generally the case in geomagnetically disturbed conditions, typically also resulting in aurora. This would explain why FAEs are observed alongside aurora. Particularly at high latitudes, these instabilities can result in significant local electron heating. This is consistent with the low-altitude elevated electron temperatures observed during the FAE events, for which Farley-Buneman instabilities are the most likely explanation.

The observed large ion temperatures in the F-region around 190 km height are caused by Joule heating from strong electric fields, or ion-neutral friction. The measurements are used to estimate the electric field strength below assuming that $E_{\parallel} = 0$, i.e. the magnetic field-lines are equipotentials. We neglect the effect of the slightly different magnetic field strengths between 190 km height and the lower E-region, and also any differences of the neutral wind between these altitudes. The ion energy balance, neglecting also thermal energy transfer to/from electrons (whose temperatures are generally not enhanced above the E-region, especially preceding the FAE occurrence at 18:23 UT) is (Alcayde et al., 1983, Equation (4)):

$$Q_{in} = \nu_{in} N_n N_e \left(\frac{3}{2} k_B \left(T_n - T_i\right) + \frac{1}{2} m_i \left(\boldsymbol{V}_i - \boldsymbol{V}_n\right)^2 \right) \tag{1}$$

Here T_i and T_n are the ion and neutral temperatures, $\boldsymbol{V}_i$ and $\boldsymbol{V}_n$ the ion and neutral drifts, respectively. m_i is the mean ion mass, k_B the Boltzmann constant, ν_{in} the ion-neutral collision frequency, and N_n and N_e the neutral and electron densities. In the steady state $Q_{in} = 0$, and for the F-region we insert $(\boldsymbol{V}_i - \boldsymbol{V}_n) = \boldsymbol{E}_\perp \times \boldsymbol{B}/B^2$ with $\boldsymbol{E}_\perp$ the electric field in the frame of the neutral gas and $\boldsymbol{B}$ the geomagnetic field. We are only interested in the magnitude of $\boldsymbol{E}_\perp$, ~~$E_\perp$. It~~ which can be estimated as

$$E_\perp / B = \sqrt{3 k_B \left(T_i - T_n\right) / m_i} \tag{2}$$

Filtering out elevated ion temperatures above 1500 K, we use the ESR data to estimate a mean background ion temperature in the quiet state of ∼950 K for the altitude range of 150–300 km, which should then approximately correspond to the neutral temperature. For m_i we use conservatively 30 amu, corresponding to a mixture between N_2^+ and O_2^+, negelecting a contribution by O^+. The motivation is that high T_i and large drift difference $|\boldsymbol{V}_i - \boldsymbol{V}_n|$ probably enhance the relative molecular concentration compared to model values as the International Reference Ionosphere (IRI) would give it. ~~The estimate, using~~ Using average elevated $T_i \approx 3300$ K for the altitude range of 150–300 km from the ESR measurement, the estimated lower limit is $E_\perp \approx 70$ mVm^{-1}. This value is far above the threshold for Farley-Buneman instabilities, which is typically around 30 mVm^{-1} (Williams et al., 1992). If molecular ions were assumed to be dominant, it would only further increase the lower limit. It should be noted that this is an approximation and the filtering for average values is based on somewhat arbitrary choices, but the derived $E_\perp$ is not all that dependent on the inserted T_i and T_n and ~~should~~ would exceed the typical limit for Farley-Buneman instabilities by a significant margin regardless of the exact filtering values. The threshold may be already exceeded in the arc, before 18:23 UT, but T_e was perhaps not high enough to excite optical emissions. Buchert et al. (2008) showed an example with the ESR where T_e reaches temperatures above 3000 K at 100-109 km, which is enough to produce 630.0 nm optical emissions according to Gustavsson et al. (2001). An open question is whether these instabilities can produce large enough T_e increases to excite all observed FAE emissions. Buchert et al. (2008) showed that T_i increased already above $\sim$125 km, up to about 4000 km. These ~~events~~ temperature enhancements are stronger than those ~~shown~~ observed at auroral oval latitudes over mainland Norway by Williams et al. (1992). This could be because at the edge of the auroral oval over Svalbard E-fields ~~are~~ may be larger than in the auroral zone, or because the ESR is more sensitive than the EISCAT mainland radar ~~back~~ was in 1992. If E-fields (and associated T_e enhancements) are typically larger at Svalbard, this might perhaps explain why FAEs have not been noticed earlier in the auroral zone or the Scandinavian mainland. Another possible contributing factor could be that auroral all-sky cameras used for scientific purposes ~~can be somewhat~~ are often more limited in pixel resolution compared to the Sony α7S used in the present study, which could reduce the likelihood of unexpectedly identifying small-scale and short-lived features like FAEs.

Whereas specific characteristics for the individually occurring FAEs are hard to identify, category 2 FAE groups with regular spacing clearly suggest a link to wave activity. We tentatively suggest that waves modulate the electric field strength and correspondingly the intensity of Farley-Buneman induced plasma turbulence and electron heating near the arcs to produce the observed category 2 FAE groups. As these groups show regular and fairly stable distances between the individual FAEs, some kind of monochromatic wave seems to be responsible. Suzuki et al. (2009) describe the modulation of airglow by gravity waves, which is similar to the modulation of category 2 FAE groups, albeit at larger scales. The short distances between FAEs suggests waves with small wavelengths. The estimated FAE drift speed of $\sim$1 km/s is much faster than the average ionospheric convection speed of a few hundred m/s. If category 2 FAEs are indeed modulated by waves, they could propagate with their phase velocity and thus exceed typical convection speeds. Alternatively the E-field modulation could originate from the magnetosphere. A candidate mechanism is that the shear between the strong flow in the high E-field adjacent to the arc and the slower flow in the arc itself leads to a Kelvin-Helmholz instability, whose phase speed would be between the slow and fast flows (see, e.g., Keskinen et al. (1988)). For $E_\perp \approx 70$ mVm^{-1}, corresponding to 1400 m/s, the phase speed of Kelvin-Helmholtz waves would be several hundred m/s, which is roughly the observed value. It is, however, unclear why the auroral arc shows no signature of the modulation, and what determines the wavelength of the quasi-periodic FAEs of $\sim$6 km.

~~Gallardo-Lacourt et al. (2018) suggest STEVE as another locally generated skyglow without any associated particle precipitation. The phenomenon is far from well-understood and occurs on much larger scales than FAEs, but indicates that ionospheric processes can indeed cause emission without particle precipitation being present. We suggest that FAEs fall within the same category, even though many of their properties such as size and lifetime differ majorly. The underlying processes heating the plasma are unlikely to be the same, but on a fundamental level both emissions seem to be related to thermal ionospheric processes rather than particle precipitation.~~

To determine a link between FAEs and other aurora-like features like STEVE or the green "streaks", and to further analyse FAE characteristics, more events will need to be studied, ideally from multiple locations and with ionospheric plasma measurements. The limited sample size, not necessarily of FAEs, but rather observation nights and ESR data for the present study, limits the conclusions that can be drawn for the underlying generation mechanism. Until these conditions are determined, FAE occurrences will be seemingly random, further complicating a targeted follow-up study.

5 Conclusions

The focus of the present study is to ~~present~~ characterise a new type of aurora-like phenomenon, which we name Fragmented Aurora-like Emissions (FAEs)~~, and analyse their basic characteristics~~. In summary, the observed FAEs can be grouped into two categories: individually occurring FAEs and groups close to auroral arcs with wave-like structure. All FAEs show a lack of field-aligned extent and seem to generally occur in the shape of an elongated ellipse. The majority of the observed FAEs have a major axis smaller than 20 km (assuming an altitude of $\sim$110 km), with a mean aspect ratio of $\sim$2. Photometer data show distinctly enhanced intensities at the 557.7 nm emission of atomic oxygen for FAEs passing the FOV, but no clear FAE signatures at the 427.8 nm and 630.0 nm wavelengths, of which the latter is not surprising, as it would be heavily collisionally quenched at the proposed altitude. A FAE signature is also clearly visible in the ASK1 673.0 nm emission channel of the first positive band system of N_2, but not at the 777.4 nm emission of atomic oxygen measured by ASK3, which together sets a range of states with different energies that ~~seem to be~~ are excitable by the generation mechanism~~or with too high of an energy threshold, respectively~~. The apparent lack of 427.8 nm and 777.4 nm emissions indicates an upper energy limit between $\sim$8–11 eV which the generation mechanism can produce. The ESR data suggest that FAEs are associated with significantly elevated electron temperatures around 110–120 km, for which Farley-Buneman instabilities are the only known cause at these low altitudes. Simultaneously, increased ion temperatures are visible at altitudes in the F-region, which enables us to estimate the strength of the E-field. The derived estimate of $E_\perp \approx 70\ \mathrm{mVm}^{-1}$ exceeds the typical Farley-Buneman threshold of 30 mVm^{-1}. Category 2 FAE groups show a fairly regular and stable spacing and appear to be modulated by some kind of wave.

Open questions are the exact nature of the generation mechanism, whether FAEs of categories 1 and 2 are caused by the same mechanism, if category 2 FAEs are indeed modulated by wave activity and if so by what kind of wave, whether they are exclusively a high-latitude phenomenon and what threshold values of ionospheric parameters are necessary for FAE occurrences.

Data availability. ACE data are available on the website of the ACE Science Center (http://www.srl.caltech.edu/ACE/ASC/). DSCOVR data are available from the NOAA Space Weather Predicition Center (http://doi.org/10.7289/V51Z42F7). SuperDARN data are available on the website of Virginia Tech (http://vt.superdarn.org/). ASC and MSP data are available from the KHO website (kho.unis.no). ASK data are availble from the ASK teams at KTH Stockholm, Sweden and the University of Southampton, UK. EISCAT data can be downloaded from the MADRIGAL database: http://portal.eiscat.se/madrigal/

Video supplement. Whiter (2020) provides access to the ASK video on which Figure 5 is based.

Author contributions. JD analysed the data set and wrote the present study. NP contributed towards the entire writing and analysis process. DW suggested the FAE name and contributed towards the writing and data analysis process, especially regarding the ASK data. PGE originally discovered the FAEs in ASC images and contributed towards the writing and data analysis process, especially regarding the ASC and MSP data. LB contributed towards the ESR data analysis and respective section. SSB suggested Farley-Buneman instabilities as a potential generation mechanism and contributed the respective discussion section.

Competing interests. NP and DW are editors for the special issue this paper has been submitted to.

Disclaimer. This study is based on J. Dreyer's master's thesis (http://urn.kb.se/resolve?urn=urn:nbn:se:uu:diva-388546), which in parts contains some additional information that might be of interest.

Acknowledgements. FAEs were independently identified in ASK data by Hanna Sundberg for an event in 2013.

JD is thankful for being supported by the Swedish National Space Agency under grant Dnr 143/18. The work by NP & LB is supported by the Norwegian Research Council (NRC) under CoE contract 223252. DW is supported by the Natural Environment Research Council (NERC, UK) under grant NE/S015167/1. ASK has been supported by NERC of the UK under grants NE/H024433/1, NE/N004051/1 and NE/S015167/1.

The authors thank the KHO team and PI Dag Lorentzen for maintenance and calibration of the Sony camera and MSP.

SuperDARN is a collection of radars funded by the national scientific funding agencies of Australia, Canada, China, France, Japan, Norway, South Africa, United Kingdom, and United States of America.

EISCAT is an international association supported by research organisations in China (CRIRP), Finland (SA), Japan (NIPR and ISEE), Norway (NFR), Sweden (VR), and the United Kingdom (UKRI).

References

Alcayde, D., Fontanari, J., Bauer, P., and de La Beaujardiere, O.: Some properties of the auroral thermosphere inferred from initial EISCAT observations, Radio Science, 18, 881–886, https://doi.org/10.1029/RS018i006p00881, 1983.

Ashrafi, M.: ASK: Auroral Structure and Kinetics in action, Astronomy & Geophysics, 48, 4.35–4.37, https://doi.org/10.1111/j.1468-4004.2007.48435.x, https://doi.org/10.1111/j.1468-4004.2007.48435.x, 2007.

Ashrafi, M., Lanchester, B. S., Lummerzheim, D., Ivchenko, N., and Jokiaho, O.: Modelling of $N_2$1P emission rates in aurora using various cross sections for excitation, Annales Geophysicae, 27, 2545–2553, https://doi.org/10.5194/angeo-27-2545-2009, https://angeo.copernicus.org/articles/27/2545/2009/, 2009.

Buchert, S. C., Tsuda, T., Fujii, R., and Nozawa, S.: The Pedersen current carried by electrons: a non-linear response of the ionosphere to magnetospheric forcing, Annales Geophysicae, 26, 2837–2844, https://doi.org/10.5194/angeo-26-2837-2008, https://angeo.copernicus.org/articles/26/2837/2008/, 2008.

Chen, X.-C., Lorentzen, D., Moen, J., Oksavik, K., and Baddeley, L.: Simultaneous ground-based optical and HF radar observations of the ionospheric footprint of the open/closed field line boundary along the geomagnetic meridian, Journal of Geophysical Research A: Space Physics, 120, 9859–9874, 2015.

Cranmer, S. R.: Coronal Holes and the High-Speed Solar Wind, Space Science Reviews, 101, 229–294, 2002.

Dahlgren, H., Ivchenko, N., Sullivan, J., Lanchester, B. S., Marklund, G., and Whiter, D.: Morphology and dynamics of aurora at fine scale: first results from the ASK instrument, Annales Geophysicae, 26, 1041–1048, https://doi.org/10.5194/angeo-26-1041-2008, 2008.

Dahlgren, H., Lanchester, B. S., Ivchenko, N., and Whiter, D. K.: Electrodynamics and energy characteristics of aurora at high resolution by optical methods, Journal of Geophysical Research: Space Physics, 121, 5966–5974, https://doi.org/10.1002/2016JA022446, https://agupubs.onlinelibrary.wiley.com/doi/abs/10.1002/2016JA022446, 2016.

Gallardo-Lacourt, B., Liang, J., Nishimura, Y., and Donovan, E.: On the Origin of STEVE: Particle Precipitation or Ionospheric Skyglow?, Geophysical Research Letters, 45, 7968–7973, https://doi.org/10.1029/2018GL078509, https://agupubs.onlinelibrary.wiley.com/doi/abs/10.1029/2018GL078509, 2018.

Gillies, D. M., Donovan, E., Hampton, D., Liang, J., Connors, M., Nishimura, Y., Gallardo-Lacourt, B., and Spanswick, E.: First Observations From the TREx Spectrograph: The Optical Spectrum of STEVE and the Picket Fence Phenomena, Geophysical Research Letters, 46, 7207–7213, https://doi.org/10.1029/2019GL083272, 2019.

Goodbody, B.: Radar and optical studies of small scale features in the Aurora: the association of optical signatures with Naturally Enhanced Ion Acoustic Lines (NEIALs), https://eprints.soton.ac.uk/365486/, 2014.

Gustavsson, B., Sergienko, T., Rietveld, M. T., Honary, F., Steen, Å., Brändström, B. U. E., Leyser, T. B., Aruliah, A. L., Aso, T., Ejiri, M., and Marple, S.: First tomographic estimate of volume distribution of HF-pump enhanced airglow emission, Journal of Geophysical Research, 106, 29 105–29 124, https://doi.org/10.1029/2000JA900167, 2001.

Hallinan, T. J., Stenbaek-Nielsen, H. C., and Deehr, C. S.: Enhanced Aurora, Journal of Geophysical Research, 90, 8461–8476, https://doi.org/10.1029/JA090iA09p08461, 1985.

Holma, H., Kaila, K. U., Kosch, M. J., and Rietveld, M. T.: Recognizing the blue emission in artificial aurora, Advances in Space Research, 38, 2653–2658, https://doi.org/10.1016/j.asr.2005.07.036, 2006.

Humberset, B. K., Gjerloev, J. W., Mann, I. R., Michell, R. G., and Samara, M.: On the Persistent Shape and Coherence of Pulsating Auroral Patches, Journal of Geophysical Research: Space Physics, 123, 4272–4289, https://doi.org/10.1029/2017JA024405, 2018.

Karlsson, T., Andersson, L., Gillies, D. M., Lynch, K., Marghitu, O., Partamies, N., Sivadas, N., and Wu, J.: Quiet, Discrete Auroral Arcs—Observations, Space Science Reviews, 216, 16, https://doi.org/10.1007/s11214-020-0641-7, https://doi.org/10.1007/s11214-020-0641-7, 2020.

Keskinen, M. J., Mitchell, H. G., Fedder, J. A., Satyanarayana, P., Zalesak, S. T., and Huba, J. D.: Nonlinear evolution of the Kelvin-Helmholtz instability in the high-latitude ionosphere, Journal of Geophysical Research: Space Physics, 93, 137–152, https://doi.org/10.1029/JA093iA01p00137, https://agupubs.onlinelibrary.wiley.com/doi/abs/10.1029/JA093iA01p00137, 1988.

Lanchester, B. S., Ashrafi, M., and Ivchenko, N.: Simultaneous imaging of aurora on small scale in OI (777.4 nm) and $N_2$1P to estimate energy and flux of precipitation, Annales Geophysicae, 27, 2881–2891, https://doi.org/10.5194/angeo-27-2881-2009, 2009.

Liu, J., Wang, W., Oppenheim, M., Dimant, Y., Wiltberger, M., and Merkin, S.: Anomalous electron heating effects on the E region ionosphere in TIEGCM, Geophysical Research Letters, 43, 2351–2358, https://doi.org/10.1002/2016GL068010, https://agupubs.onlinelibrary.wiley.com/doi/abs/10.1002/2016GL068010, 2016.

MacDonald, E. A., Donovan, E., Nishimura, Y., Case, N. A., Gillies, D. M., Gallardo-Lacourt, B., Archer, W. E., Spanswick, E. L., Bourassa, N., Connors, M., Heavner, M., Jackel, B., Kosar, B., Knudsen, D. J., Ratzlaff, C., and Schofield, I.: New science in plain sight: Citizen scientists lead to the discovery of optical structure in the upper atmosphere, Science Advances, 4, https://doi.org/10.1126/sciadv.aaq0030, https://advances.sciencemag.org/content/4/3/eaaq0030, 2018.

McKay, D., Paavilainen, T., Gustavsson, B., Kvammen, A., and Partamies, N.: Lumikot: Fast Auroral Transients During the Growth Phase of Substorms, Geophysical Research Letters, 46, 7214–7221, https://doi.org/10.1029/2019GL082985, https://agupubs.onlinelibrary.wiley.com/doi/abs/10.1029/2019GL082985, 2019.

Mende, S. B. and Turner, C.: Color Ratios of Subauroral (STEVE) Arcs, Journal of Geophysical Research: Space Physics, 124, 5945–5955, https://doi.org/https://doi.org/10.1029/2019JA026851, https://agupubs.onlinelibrary.wiley.com/doi/abs/10.1029/2019JA026851, 2019.

Mende, S. B., Harding, B. J., and Turner, C.: Subauroral Green STEVE Arcs: Evidence for Low-Energy Excitation, Geophysical Research Letters, 46, 14 256–14 262, https://doi.org/https://doi.org/10.1029/2019GL086145, https://agupubs.onlinelibrary.wiley.com/doi/abs/10.1029/2019GL086145, 2019.

Nishimura, Y., Gallardo-Lacourt, B., Zou, Y., Mishin, E., Knudsen, D. J., Donovan, E. F., Angelopoulos, V., and Raybell, R.: Magnetospheric Signatures of STEVE: Implications for the Magnetospheric Energy Source and Interhemispheric Conjugacy, Geophysical Research Letters, 46, 5637–5644, https://doi.org/10.1029/2019GL082460, https://agupubs.onlinelibrary.wiley.com/doi/abs/10.1029/2019GL082460, 2019.

Nishimura, Y., Lessard, M. R., Katoh, Y., Miyoshi, Y., Grono, E., Partamies, N., Sivadas, N., Hosokawa, K., Fukizawa, M., Samara, M., Michell, R. G., Kataoka, R., Sakanoi, T., Whiter, D. K., ichiro Oyama, S., Ogawa, Y., and Kurita, S.: Diffuse and Pulsating Aurora, Space Science Reviews, 216, 1–38, https://doi.org/10.1007/s11214-019-0629-3, http://dx.doi.org/10.1007/s11214-019-0629-3, 2020.

Oppenheim, M., Otani, N., and Ronchi, C.: Saturation of the Farley-Buneman instability via nonlinear electron E×B drifts, Journal of Geophysical Research: Space Physics, 101, 17 273–17 286, 1996.

Palmroth, M., Grandin, M., Helin, M., Koski, P., Oksanen, A., Glad, M. A., Valonen, R., Saari, K., Bruus, E., Norberg, J., Viljanen, A., Kauristie, K., and Verronen, P. T.: Citizen Scientists Discover a New Auroral Form: Dunes Provide Insight Into the Upper Atmosphere, AGU Advances, 1, e2019AV000 133, https://doi.org/10.1029/2019AV000133, https://agupubs.onlinelibrary.wiley.com/doi/abs/10.1029/2019AV000133, e2019AV000133 aga2.20017, 2019.

Peverall, R., Rosén, S., Larsson, M., Peterson, J. R., Bobbenkamp, R., Guberman, S. L., Danared, H., af Ugglas, M., Al-Khalili, A., Maurellis, A. N., and van der Zande, W. J.: The ionospheric oxygen Green airglow: Electron temperature dependence and aeronomical implications, Geophysical Research Letters, 27, 481–484, https://doi.org/10.1029/1999GL010711, https://agupubs.onlinelibrary.wiley.com/doi/abs/10.1029/1999GL010711, 2000.

Rueden, C. T., Schindelin, J., Hiner, M. C., DeZonia, B. E., Walter, A. E., Arena, E. T., and Eliceiri, K. W.: ImageJ2: ImageJ for the next generation of scientific image data, BMC Bioinformatics, 18, 529, https://doi.org/10.1186/s12859-017-1934-z, https://doi.org/10.1186/s12859-017-1934-z, 2017.

Schindelin, J., Arganda-Carreras, I., Frise, E., Kaynig, V., Longair, M., Pietzsch, T., Preibisch, S., Rueden, C., Saalfeld, S., Schmid, B., Tinevez, J.-Y., White, D. J., Hartenstein, V., Eliceiri, K., Tomancak, P., and Cardona, A.: Fiji: an open-source platform for biological-image analysis, Nature Methods, 9, 676–682, https://doi.org/10.1038/nmeth.2019, http://www.nature.com/articles/nmeth.2019, 2012.

Semeter, J., Hunnekuhl, M., MacDonald, E., Hirsch, M., Zeller, N., Chernenkoff, A., and Wang, J.: The Mysterious Green Streaks Below STEVE, AGU Advances, 1, e2020AV000 183, https://doi.org/https://doi.org/10.1029/2020AV000183, https://agupubs.onlinelibrary.wiley.com/doi/abs/10.1029/2020AV000183, e2020AV000183 10.1029/2020AV000183, 2020.

Suzuki, S., Shiokawa, K., Liu, A. Z., Otsuka, Y., Ogawa, T., and Nakamura, T.: Characteristics of equatorial gravity waves derived from mesospheric airglow imaging observations, Annales Geophysicae, 27, 1625–1629, https://doi.org/10.5194/angeo-27-1625-2009, https://angeo.copernicus.org/articles/27/1625/2009/, 2009.

Wannberg, G., Wolf, I., Vanhainen, L. ., Koskenniemi, K., Röttger, J., Postila, M., Markkanen, J., Jacobsen, R., Stenberg, A., Larsen, R., Eliassen, S., Heck, S., and Huuskonen, A.: The EISCAT Svalbard radar: A case study in modern incoherent scatter radar system design, Radio Science, 32, 2283–2307, 1997.

Whiter, D.: Auroral Structure and Kinetics video observations from Longyearbyen, Svalbard, 2015/12/07, 18:23UT, https://eprints.soton.ac.uk/441916/, 2020.

Williams, P., Jones, B., and Jones, G.: The measured relationship between electric field strength and electron temperature in the auroral E-region, Journal of Atmospheric and Terrestrial Physics, 54, 741 – 748, https://doi.org/https://doi.org/10.1016/0021-9169(92)90112-X, http://www.sciencedirect.com/science/article/pii/002191699290112X, e-Region Irregularities, 1992.